Am J Cancer Res 2024;14(2):917-930
www.ajcr.us /ISSN:2156-6976/ajcr0155138

Original Article

PPIB/Cyclophilin B expression associates with tumor progression and unfavorable survival in patients with pulmonary adenocarcinoma

Ilseon Hwang[1*], Joon Seon Song[2*], Eunho Cho[3,4,5*], Kwon-Ho Song[6], Sang Hyun Ra[7], Chang-Min Choi[8], Tae Woo Kim[3,4,5], Sung-Han Kim[7], Jeong Won Kim[9], Joon-Yong Chung[10]

[1]Department of Pathology, Keimyung University School of Medicine, Dongsan Medical Center, Daegu 42601, Republic of Korea; [2]Department of Pathology, Asan Medical Center, University of Ulsan College of Medicine, Seoul 05505, Republic of Korea; [3]Department of Biochemistry and Molecular Biology, Korea University College of Medicine, Seoul 02841, Republic of Korea; [4]Department of Biomedical Science, Korea University College of Medicine, Seoul 02841, Republic of Korea; [5]BK21 Graduate Program, Department of Biomedical Science, Korea University College of Medicine, Seoul 02841, Republic of Korea; [6]Department of Cell Biology, Daegu Catholic University School of Medicine, Daegu 42472, Republic of Korea; [7]Department of Infectious Diseases, Asan Medical Center, University of Ulsan College of Medicine, Seoul 05505, Republic of Korea; [8]Department of Pulmonary and Critical Care Medicine and Oncology, Asan Medical Center, University of Ulsan College of Medicine, Seoul 05505, Republic of Korea; [9]Department of Pathology, Kangnam Sacred Heart Hospital, Hallym University College of Medicine, Seoul 07441, Republic of Korea; [10]Molecular Imaging Branch, Center for Cancer Research, National Cancer Institute, National Institutes of Health, Bethesda, MD 20852, USA. [*]Equal contributors.

Received December 27, 2023; Accepted February 22, 2024; Epub February 25, 2024; Published February 28, 2024

Abstract: Cyclophilin B (CypB), encoded by peptidylprolyl isomerase B (*PPIB*), is involved in cellular transcriptional regulation, immune responses, chemotaxis, and proliferation. Recent studies have shown that PPIB/CypB is associated with tumor progression and chemoresistance in various cancers. However, the clinicopathologic significance and mechanism of action of PPIB/CypB in non-small cell lung cancer (NSCLC) remain unclear. In this study, we used RNA in situ hybridization to examine PPIB expression in 431 NSCLC tissue microarrays consisting of 295 adenocarcinomas (ADCs) and 136 squamous cell carcinomas (SCCs). Additionally, Ki-67 expression was evaluated using immunohistochemistry. The role of PPIB/CypB was assessed in five human NSCLC cell lines. There was a significant correlation between PPIB/CypB expression and Ki-67 expression in ADC (Spearman correlation r=0.374, P<0.001) and a weak correlation in SCC (r=0.229, P=0.007). In ADCs, high PPIB expression (PPIB^{high}) was associated with lymph node metastasis (P=0.023), advanced disease stage (P=0.014), disease recurrence (P=0.013), and patient mortality (P=0.015). Meanwhile, high Ki-67 expression (Ki-67^{high}) was correlated with male sex, smoking history, high pT stage, lymph node metastasis, advanced stage, disease recurrence, and patient mortality in ADC (all P<0.001). However, there was no association between either marker or clinicopathological factors, except for old age and PPIB^{high} (P=0.038) in SCC. Survival analyses revealed that the combined expression of PPIB^{high}/Ki-67^{high} was an independent prognosis factor for poor disease-free survival (HR 1.424, 95% CI 1.177-1.723, P<0.001) and overall survival (HR 1.266, 95% CI 1.036-1.548, P=0.021) in ADC, but not in SCC. Furthermore, PPIB/CypB promoted the proliferation, colony formation, and migration of NSCLC cells. We also observed the oncogenic properties of PPIB/CypB expression in human bronchial epithelial cells. In conclusion, PPIB/CypB contributes to tumor growth in NSCLC, and elevated PPIB/Ki-67 levels are linked to unfavorable survival, especially in ADC.

Keywords: Peptidylprolyl isomerase B, Ki-67, prognosis, non-small cell lung cancer, adenocarcinoma

Introduction

Lung cancer is the leading cause of cancer-associated deaths worldwide, with non-small cell lung carcinoma (NSCLC) accounting for approximately 85% of lung cancer cases [1]. In the United States, the 5-year relative survival rate of NSCLC is 26%, which remains low despite recent improvements [2]. The tumor, node, and metastasis (TNM) staging system, endorsed by both the International Association for the Study of Lung Cancer (IASLC) and the

https://doi.org/10.62347/TYNU2341

American Joint Committee on Cancer (AJCC), has been internationally employed to classify the extent and its correlation with survival outcomes. Adenocarcinoma (ADC), the most common histological type, and squamous cell carcinoma, another common subtype, are the two major subtypes of NSCLCs, accounting for more than 85% of the cases [3]. As they exhibit distinct characteristics, including differences in the origin of tumor cells, location, specific biomarkers, and oncogenic drivers [4], the histopathologic subtype has become a crucial factor in NSCLC patient survival and in guiding their therapeutic plan [5, 6]. Additionally, the Ki-67 labeling index is a well-established histological marker for predicting the survival of patients with NSCLC [7].

Cyclophilins, a cyclophilin family of peptidylprolyl *cis*-trans isomerases, have been identified as abundant intracellular binding proteins with a high affinity for the immunosuppressant cyclosporin A. They contribute to diverse cellular functions, including transcriptional regulation, immune response, chemotaxis, protein secretion, protein folding and trafficking, and regulation of mitochondrial permeability [8]. Cyclophilin B (CypB), encoded by peptidylprolyl isomerase B (*PPIB*) and primarily located in the endoplasmic reticulum, has been highly conserved throughout evolution, indicating that it plays an important role as a housekeeping gene [9]. In pathological conditions, PPIB/CypB plays a role in hepatitis C replication [10] and has also been reported to be involved in the tumorigenesis of various cancers, including hepatocellular carcinoma, gastric cancer, breast cancer, cervical cancer, head and neck squamous cell carcinoma, and glioblastoma [11-16]. Furthermore, PPIB/CypB has been implicated in conferring resistance to certain anticancer agents such as cisplatin and oxaliplatin [17, 18]. However, the role of PPIB/CypB in NSCLC development and its underlying molecular mechanisms remain elusive. The clinicopathological significance of PPIB expression in NSCLC also remains unclear.

The aim of the present study was to explore the clinicopathologic significance of PPIB expression in ADC and SCC, common subtypes of NSCLCs, and to elucidate the underlying functional mechanisms responsible for inducing of PPIB/CypB expression in NSCLC cell lines.

Materials and methods

Patients and tissue samples

A total of 431 surgically resected primary NSCLC specimens obtained between January 2011 and December 2011 were retrieved from the Department of Pathology at Asan Medical Center, Seoul, Korea. Clinical data, including age, sex, smoking history, adjuvant chemotherapy, survival status, and survival time of patients, and pathological data, including histologic type, differentiation, and pTNM classification, were collected from medical records and pathologic reports. The NSCLC cohort included 295 patients with ADCs and 136 patients with SCCs. Patients with other histological types, such as small cell carcinoma, large cell neuroendocrine carcinoma, large cell carcinoma, adenosquamous cell carcinoma, and sarcomatoid carcinoma, were excluded. The histological subtypes of NSCLC were classified based on both histological findings and ancillary immunohistochemical results, such as p40, p63, TTF-1 and Napsin A according to the 2021 World Health Organization classification of histological types [19]. TNM stage was adjusted according to the 8th AJCC Staging Manual [3]. Recurrence was determined according to the Response Evaluation Criteria in Solid Tumors (RECIST; version 1.1) using computed tomography or magnetic resonance imaging. The patient status was assessed at the last follow-up visit. This study was approved by the Institutional Review Board of the Asan Medical Center (approval number: 2016-0752, Seoul, Republic of Korea), and informed consent was obtained from each patient. All procedures were conducted in accordance with the Helsinki Declaration.

RNA-in situ hybridization

RNA *in situ* hybridization for PPIB was performed using an RNAscope 2.5 detection kit with Hs-*PPIB* (Cat. No. 313901) and a negative control probe [*Bacillus subtilis* dihydrodipicolinate reductase (*DapB*)] (Cat. No. 310043) gene (Advanced Cellular Diagnostics Inc., Hayward, CA, USA), as previously described [20]. Briefly, 5-μm sectioned tissue microarray (TMA) slides were deparaffinized and pretreated with heat and protease before hybridization under standard pretreatment conditions. Slides

were incubated with Hs-PPIB or *DapB* probe for 2 h at 40°C within a humidity control chamber. Signal amplification and detection reagents were applied sequentially, according to the manufacturer's instructions. Positive signals were visualized with 3,3'-dimaniobenzadine (DAB)+ substrate-chromogen resulting in brown dots, counterstained in hematoxylin. Images were acquired using an Aperio AT2 digital scanner with a 40× objective lens (Leica Biosystems).

Captured digital images were then imported into the computer-assisted image analyzing software, Visiopharm software v6.9.1 (Visiopharm, Hørsholm, Denmark) for quantification of PPIB. After training the system by digitally "painting" examples of the nucleus in the image, tumor nuclei were defined and cytoplasm is further defined by outlining the defined nucleus. In addition, the DAB dots were identified using a Bayesian classifier trained during the preprocessing steps. The mean number of DAB dots per tumor cell in the representative area of each TMA core was calculated.

Immunohistochemical analysis

Immunohistochemistry was performed on 5-μm sectioned TMA slides. Briefly, slides were deparaffinized in xylene and graded alcohols, and the heat epitope was retrieved in a buffer (pH 9.0) containing EDTA (Dako, Carpinteria, CA, USA) using a DAKO pressure cooker. Endogenous peroxidase activity was quenched using 0.3% hydrogen peroxidase in water for 10 min. Then, the primary rabbit monoclonal Ki-67 antibody (Clone SP6; Cell Marque, Rocklin, CA, USA) was added at 1:250 for 30 min at room temperature, followed by incubation with DAKO Envision+ HRP-labeled polymer for an additional 30 min to detect the immunoenzymatic reaction. Slides were then visualized with DAB+ substrate-chromogen resulting in a brown precipitate at the antigen site, counterstained in hematoxylin and coverslipped. Rabbit isotype control immunoglobulin G (IgG) was used instead of the primary antibody to evaluate non-specific staining.

All stained slides were scanned using an Aperio AT2 digital scanner with a 40× objective lens (Leica Biosystems). The images were analyzed using Visiopharm software v6.9.1 (Visiopharm, Hørsholm, Denmark). Tumor regions were outlined manually within the region of interest (ROI) and nuclei were defined after training the system. Ki-67 expression was calculated based on the percentage of stained tumor cell nuclei.

Cells, cell culture and generation of cell lines

Human NSCLC cells (A549, PC-9, Calu-3, H460 and H2009) and immortalized human bronchial epithelial (HBE) BEAS-2B cells were purchased from the American Type Culture Collection (ATCC, Manassas, VA, USA). Non-transformed HBE 1799 cells were obtained from Dr. Y. G. Park (Seoul, Korea). All cells were tested for mycoplasma using the Mycoplasma Detection Kit (Thermo Fisher Scientific, San Jose, CA, USA) and grown at 37°C in a 5% CO_2 incubator/humidified chamber. To generate H2009-PPIB and 1799-PPIB cells, pCMV3-PPIB-FLAG plasmids (Sino Biological, Beijing, China) were transfected into the H2009 and 1799 cells. Stably transfected lines were selected and maintained in the presence of the appropriate concentrations of Hygromycin B (Duchefa Biochemistry, Haarlem, Netherlands).

siRNA constructs

Synthetic small interfering RNAs (siRNAs) specific for *GFP* and *PPIB* were purchased from Bioneer (Daejeon, Korea): Non-specific *GFP* (green fluorescent protein), 5'-GCAUCAAGGUGAACUUCAA-3' (sense), 5'-UUGAAGUUCACCUUGAUGC-3' (antisense); *PPIB-#1*, 5'-CAGCAAAUUCCAUCGUGUA-3' (sense), 5'-UACACGAUGGAAUUUGCUG-3' (antisense); *PPIB-#2*, 5'-CUUAGCUACAGGAGAGAAA-3' (sense), 5'-UUUCUCUCCUGUAGCUAAG-3' (antisense); and *PPIB-#3*, 5'-GUGUAUUUUGACCUACGAA-3' (sense), 5'-UUCGUAGGUCAAAAUACAC-3' (antisense). Cells were transfected with 100 pmol of synthesized siRNA using Lipofectamine 2000 (Invitrogen, Carlsbad, CA, USA) according to the manufacturer's instructions.

Western blot analysis

Lysates extracted from 5×10^5 cells were used for western blot analysis as described previously [21]. Primary antibodies against PPIB (101242-T36, Sino Biological), FLAG (M185-3L, MBL, Nagoya, Japan) and *β*-ACTIN (M177-3, MBL) were used in Western blot analysis, followed by the appropriate secondary antibodies conjugated with horseradish peroxidase. Immunoreactive bands were developed using

an ECL chemiluminescence detection system (Elpis Biotech, Daejeon, Korea) and signals were detected using a luminescent image analyzer (LAS-4000 Mini, Fujifilm, Tokyo, Japan). *β*-ACTIN was included as an internal loading control. The intensity of the western blot signals was quantified using Multi-gauge software (Fujifilm).

Trypan blue exclusion assay

Cell proliferation was determined using the trypan blue exclusion assay as described previously [22]. Briefly, the cells were harvested at the indicated times and stained with 0.4% trypan blue to exclude dead cells. The number of live cells was counted using a hemocytometer and a light microscope.

Flow cytometry analysis

The cells (2×10^5) were harvested by trypsinization, washed, and resuspended in PBS. To detect cellular Ki-67 expressional levels, the gathered cells were then reacted with PerCP/Cyanine5.5-conjugated anti-Ki-67 (350520, Biolegend, San Diego, CA, USA) or isotype control antibody for 1 h at 4°C. The stained cells were washed twice and analyzed using a FACSVerse flow cytometer (BD Biosciences, San Jose, CA, USA). Data were acquired using a FACSVerse flow cytometer and analyzed using BD FACSuite software (BD Biosciences).

Colony formation assay

Cells were plated onto 12-well cell culture plates and incubated for one week to allow colonies to develop. The colonies were stained with crystal violet (0.5% in methanol; Sigma-Aldrich, St. Louis, MO, USA) for 10 min and washed with deionized water to remove excess stain. Stained colonies with a diameter of 1 mm were counted manually from microscopic images. Each colony formation assay was performed in triplicate and repeated three times.

Wound-healing assay

The cell migration capacity was determined using a scratch wound healing assay. The cells were incubated in 6-well cell culture plates to obtain a confluent monolayer. The wounds were scratched using pipette tips, and the medium was replaced with fresh medium after washing the free-floating cells. Culture plates were incubated at 37°C in a CO_2 incubator, and the distance between the migrated cells was measured during this period. Photographs were taken after 24 h.

Statistical analysis

The chi-square test was used to analyze the association between the degree of PPIB or Ki-67 positivity and clinical variables (sex, smoking, differentiation, histologic type, pT stage, pN stage, recurrence, and status). An independent t-test was used to analyze PPIB or Ki-67 positivity and age. Disease-free survival (DFS) and overall survival (OS) were calculated using the Kaplan-Meier method with log-rank tests. The expression levels of PPIB and Ki-67 were dichotomized (high vs. low) using the cut-off values that provided the most discriminative power (0.8 for PPIB and 23% for Ki-67). Univariate and multivariate analyses were conducted using the Cox proportional hazards regression model to identify prognostic factors. The statistical significance level was set at 0.05. All statistical analyses were performed using IBM SPSS ver. 26.0 (SPSS Inc., Chicago, IL, USA).

Results

Clinicopathologic characteristics of patients with NSCLC

The characteristics of the 431 patients and their tumors are summarized in **Table 1**. The mean age of the patients was 63.0 years (range 35.0-86.0 years) and 68.9% of patients were males. There were 295 (68.4%) ADC and 136 (31.6 %) SCC cases. There were 281 patients (65.2%) with a history of smoking, and 97.1% of the patients with SCC had a history of smoking. For SCC, 135 (99.2%) cases were males and the mean was 65.5 years, ranging from 43.0 to 84.0 years. ADC had a much more similar sex distribution, with 162 cases (54.9%) in males and 133 (45.1%) in females. The mean age of the patients with ADC was 62.0 years, ranging from 35.0 to 86.0 years. There were 83 (19.3%), 307 (71.4%), and 40 (9.3%) well differentiated, moderately differentiated, and poorly differentiated tumors, respectively. Tumors of pT1 and pT2 were 192 (44.6%) and 141 (32.7%), respectively, whereas 98 tumors (22.7%) were classified as pT3 or higher. Lymph node and distant

Table 1. Characteristics of patients (*n*=431)

Category	No. (%)	ADC (*n*=295)	SCC (*n*=136)	*p* value
No. Age (mean, yrs)		62.0 ± 9.4	65.5 ± 8.2	<0.001*
Sex				
Male	297 (68.9)	162 (54.9)	135 (99.2)	<0.001*
Female	134 (31.1)	133 (45.1)	1 (0.73)	
Smoking				<0.001*
No	150 (34.8)	146 (49.5)	4 (2.9)	
Yes	281 (65.2)	149 (50.5)	132 (97.1)	
Differentiation				<0.001*
Well	83 (19.3)	72 (24.5)	11 (8.1)	
Moderate	307 (71.4)	213 (72.4)	94 (69.1)	
Poor	40 (9.3)	9 (3.1)	31 (22.8)	
pT stage				<0.001*
Ia-Ic	192 (44.5)	156 (52.9)	36 (26.5)	
IIa-IIb	141 (32.7)	99 (33.6)	42 (30.9)	
III-IV	98 (22.7)	40 (13.5)	58 (42.6)	
pN stage				0.071
0	295 (68.4)	210 (71.2)	85 (62.5)	
I-II	136 (31.6)	85 (28.8)	51 (37.5)	
pM stage				0.725
M0	413 (95.8)	282 (95.6)	131 (96.3)	
M1	18 (4.2)	13 (4.4)	5 (3.7)	
Stage				0.003*
I	241 (55.9)	187 (63.4)	54 (39.7)	
II	82 (19.0)	39 (13.2)	43 (31.6)	
III	90 (20.9)	56 (19.0)	34 (25.0)	
IV	18 (4.2)	13 (4.4)	5 (3.7)	
Recurrence				0.609
Absent	297 (68.9)	201 (68.1)	96 (70.6)	
Present	134 (31.1)	94 (31.9)	40 (29.4)	
Status				0.098
Alive	293 (68.0)	208 (70.5)	85 (62.5)	
Expire	138 (32.0)	87 (29.5)	51 (37.5)	
PPIB expression				0.659
Low	152 (35.3)	102 (34.6)	50 (36.8)	
High	279 (64.7)	193 (65.4)	86 (63.2)	
Ki-67 expression				<0.001*
Low	185 (42.9)	184 (62.4)	1 (0.7)	
High	246 (57.1)	111 (37.6)	135 (99.3)	

*Statistically significant (*P*<0.05).

metastases were observed in 136 (31.6%) and 18 patients (4.2%), respectively. At the time of diagnosis, 241 (55.9%), 82 (19.0%), 90 (20.9%), and 18 (4.2%) patients were categorized as having stage I, II, III, and IV disease, respectively. ADC tended to exhibit differentiated tumors (*P*<0.001), lower pT stage (*P*<0.001), and lower AJCC stage (*P*=0.003) than SCC. Tumor recurrence was recorded in 134 patients (31.1%) and 138 patients (32.0%) died. The median follow-up period was 59.9 months (range 0.1-92.3 months).

PPIB and Ki-67 expression in patients with NSCLC

Representative *in situ* hybridization images of PPIB and immunohistochemical images of Ki-67 are shown in **Figure 1** and Supplementary Figure 1, respectively. A total of 279 (64.7%) NSCLCs were classified as high PPIB-expressing cases, and 246 (57.1%) had high Ki-67 expression (Supplementary Table 1). PPIB expression was not associated with histological type; however, high Ki-67 expression was frequently observed in SCC (*P*< 0.001; **Table 1** and Supplementary Figure 2).

In analyses according to histological type, high PPIB expression in patients with ADC was significantly correlated with lymph node metastasis (*P*=0.023), advanced stage (*P*=0.014), disease recurrence (*P*=0.013), and patient mortality (*P*=0.015; **Table 2**). High Ki-67 expression was significantly associated with male sex, smoking history, high pT stage, lymph node metastasis, advanced stage, disease recurrence, and patient mortality (all *P*<0.001; **Table 2**). However, there was no association between either marker and the clinicopathological factors, except for old age and high PPIB expression (*P*=0.038) in the SCC subgroup (Supplementary Table 2).

PPIB expression in NSCLC showed a weak positive correlation with Ki-67 expression (Spearman's correlation *coefficient r*=0.191, *P*< 0.001; **Figure 2A**). In ADC, PPIB expression was

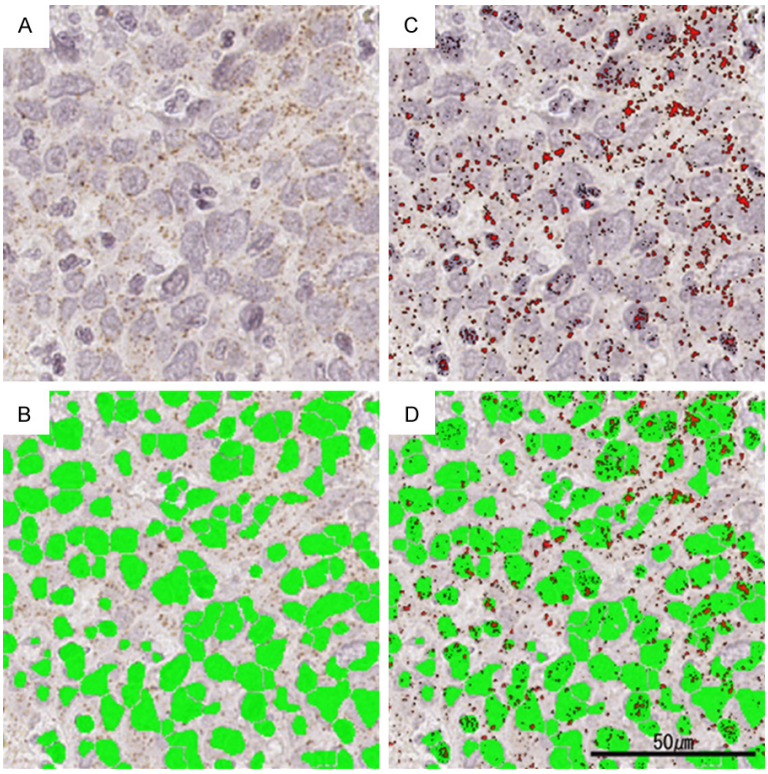

Figure 1. Assessment of PPIB expression in human NSCLC tissues. Digital images were automatically analyzed using Visiopharm software (v6.9.1) for quantification of PPIB expression. A captured RNAscope image of poorly differentiated adenocarcinoma (A) showed outlined tumor nuclei (green) (B), followed by identification of positive PPIB signals (red dots) (C). The mean value of DAB dots per tumor cells was calculated (D).

strongly correlated with Ki-67 expression (Spearman correlation r=0.374, P<0.001; **Figure 2B**), whereas there was a weak positive correlation between *PPIB* and Ki-67 expression (Spearman correlation r=0.229, P=0.007) in SCC (**Figure 2C**).

Prognostic significance of PPIB and Ki-67 expression in patients with NSCLC

Next, we assessed the relationship between PPIB and Ki-67 expression, and patient survival in 295 ADC and 136 SCC patients using available DFS and OS data. The DFS and OS of ADC patients with high PPIB expression were significantly worse than those with low PPIB expression (P=0.008 and 0.014, respectively; **Figure 3A** and **3D**). ADC patients with and high Ki-67 expression showed a significant disadvantage for DFS and OS (P<0.001; **Figure 3B** and **3E**). However, in SCC, PPIB and Ki-67 expression were not significantly associated with patient survival (Supplementary Figure 3).

After combining the results of PPIB and Ki-67 expressions in ADC, there were high PPIB/high Ki-67 ($PPIB^{high}/Ki\text{-}67^{high}$, n=87, 29.5%), low PPIB/high Ki-67 ($PPIB^{low}/Ki\text{-}67^{high}$, n=24, 8.1%), high PPIB/low Ki-67 ($PPIB^{high}/Ki\text{-}67^{low}$, n=107, 36.3%), and low PPIB/low Ki-67 ($PPIB^{low}/Ki\text{-}67^{low}$, n=77, 26.1%) expression groups. The 5-year DFS rates were 46.6%, 56.4%, 72.4%, and 85.1%, respectively (P<0.001; **Figure 3C**). In the pairwise analysis, $PPIB^{high}/Ki\text{-}67^{high}$ patients showed the worst DFS compared to those of the other groups ($PPIB^{high}/Ki\text{-}67^{high}$ *vs.* $PPIB^{high}/Ki\text{-}67^{low}$, P<0.001; $PPIB^{high}/Ki\text{-}67^{high}$ *vs.* $PPIB^{low}/Ki\text{-}67^{low}$, P<0.001; $PPIB^{low}/Ki\text{-}67^{high}$ *vs.* $PPIB^{low}/Ki\text{-}67^{low}$, P=0.008). However, there were no statistically significant differences between the other groups, including $PPIB^{high}/Ki\text{-}67^{high}$ *vs.* $PPIB^{low}/Ki\text{-}67^{high}$ (P=0.276), $PPIB^{low}/Ki\text{-}67^{high}$ *vs.* $PPIB^{high}/Ki\text{-}67^{low}$ (P=0.085), and $PPIB^{high}/Ki\text{-}67^{low}$ *vs.* $PPIB^{low}/Ki\text{-}67^{low}$ (P=0.171). The 5-year OS rate were 54.8%, 66.2%, 80.7% and 85.2%, respectively (P<0.001, **Figure 3F**). The OS of the $PPIB^{high}/Ki\text{-}67^{high}$ *vs.* $PPIB^{high}/Ki\text{-}67^{low}$ (P<0.001) groups and $PPIB^{high}/Ki\text{-}67^{high}$ *vs.* $PPIB^{low}/Ki\text{-}67^{low}$ (P<0.001) groups was significantly different.

Cox proportional analysis was performed for DFS and OS with regard to clinicopathological factors, including age, sex, pT stage, pN stage, PPIB, and Ki-67 expression (**Tables 3** and **4**). Among these, high pT stage (P<0.001), high pN stage (P<0.001), high PPIB expression (P=0.009), high Ki-67 expression (P<0.001), and $PPIB^{high}/Ki\text{-}67^{high}$ (P<0.001) were associated with significantly worse DFS in univariate analysis. Old age (P=0.005), male sex (P=0.038), high pT stage (P=0.001), high pN stage (P<0.001), high PPIB expression (P=0.015), high Ki-67 expression (P<0.001), and $PPIB^{high}/Ki\text{-}67^{high}$ (P<0.001) were significantly correlated with shorter OS. In multivariate anal-

Table 2. Association of *PPIB* and Ki-67 expression with clinicopathologic characteristics in pulmonary adenocarcinoma

Category	*PPIB*, No. (%)			Ki-67, No. (%)		
	Low (<0.8, *n*=102)	High (≥0.8, *n*=193)	*p* value	Low (<23.0, *n*=184)	High (≥23.0, *n*=111)	*p* value
Age	61.8 ± 8.7	62.1 ± 9.8	0.814	61.4 ± 9.1	62.9 ± 9.9	0.203
Sex			0.217			<0.001*
Male	51 (50)	111 (57.5)		86 (46.7)	76 (68.4)	
Female	51 (50)	82 (42.4)		98 (53.2)	35 (31.5)	
Smoking			0.110			<0.001*
No	57 (55.8)	89 (46.1)		110 (59.7)	36 (32.4)	
Yes	45 (44.1)	104 (53.8)		74 (40.2)	75 (67.5)	
Differentiation[a]			0.422			<0.001*
Well	28 (27.4)	44 (22.9)		61 (33.1)	11 (10)	
Moderate	71 (69.6)	142 (73.9)		121 (65.7)	92 (83.6)	
Poor	3 (2.94)	6 (3.12)		2 (1.08)	7 (6.36)	
pT stage			0.313			<0.001*
Ia-Ic	58 (56.8)	98 (50.7)		114 (61.9)	42 (37.8)	
IIa-IIb	32 (31.3)	67 (34.7)		53 (28.8)	46 (41.4)	
III-IV	12 (11.7)	28 (14.5)		17 (9.23)	23 (20.7)	
pN stage			0.023*			<0.001*
0	81 (79.4)	129 (66.8)		150 (81.5)	60 (54.0)	
I-II	21 (20.5)	64 (33.1)		34 (18.4)	51 (45.9)	
pM stage			0.231			0.248
M0	100 (98.0)	182 (94.3)		178 (96.7)	104 (93.6)	
M1	2 (1.96)	11 (5.69)		6 (3.26)	7 (6.30)	
Stage			0.014*			<0.001*
I	71 (69.6)	116 (60.1)		138 (75.0)	49 (44.1)	
II	17 (16.6)	22 (11.3)		18 (9.78)	21 (18.9)	
III	12 (11.7)	44 (22.7)		22 (11.9)	34 (30.6)	
IV	2 (1.96)	11 (5.69)		6 (3.26)	7 (6.30)	
Recurrence			0.013*			<0.001*
Absent	79 (77.4)	122 (63.2)		143 (77.7)	58 (52.2)	
Present	23 (22.5)	71 (36.7)		41 (22.2)	53 (47.7)	
Status			0.015*			<0.001*
Alive	81 (79.4)	127 (65.8)		145 (78.8)	63 (56.7)	
Expire	21 (20.5)	66 (34.1)		39 (21.1)	48 (43.2)	

[a]Calculated with only 294 cases with available information on tumor grade. *Statistically significant (*P*<0.05).

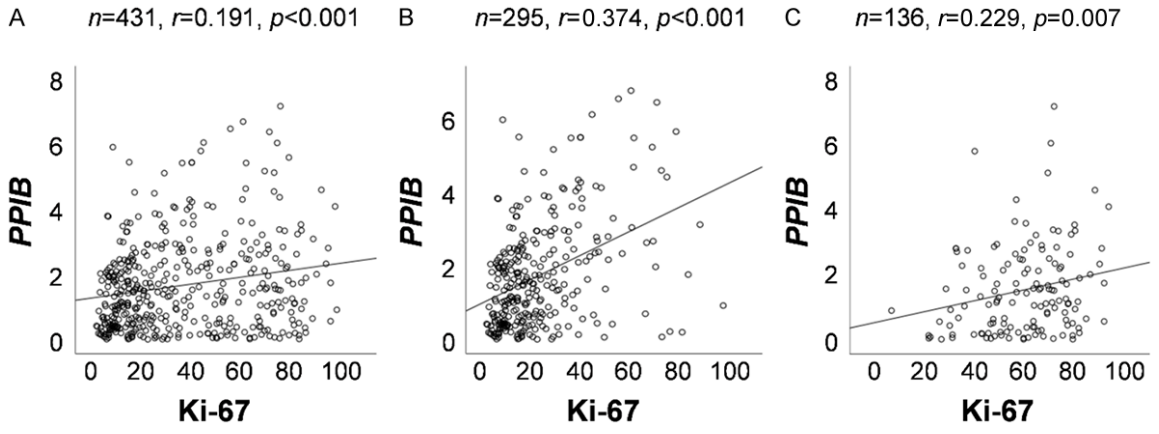

Figure 2. Correlation analysis between PPIB and Ki-67 expression in NSCLC (A), adenocarcinoma (ADC) group (B), and squamous cell carcinoma (SCC) group (C). PPIB expression showed a significant positive correlation with Ki-67 in ADC (Spearman correlation *r*=0.374, *P*<0.001), but a weak correlation in all NSCLC (Spearman correlation *r*=0.191, *P*<0.001) and SCC (Spearman correlation *r*=0.229, *P*=0.007).

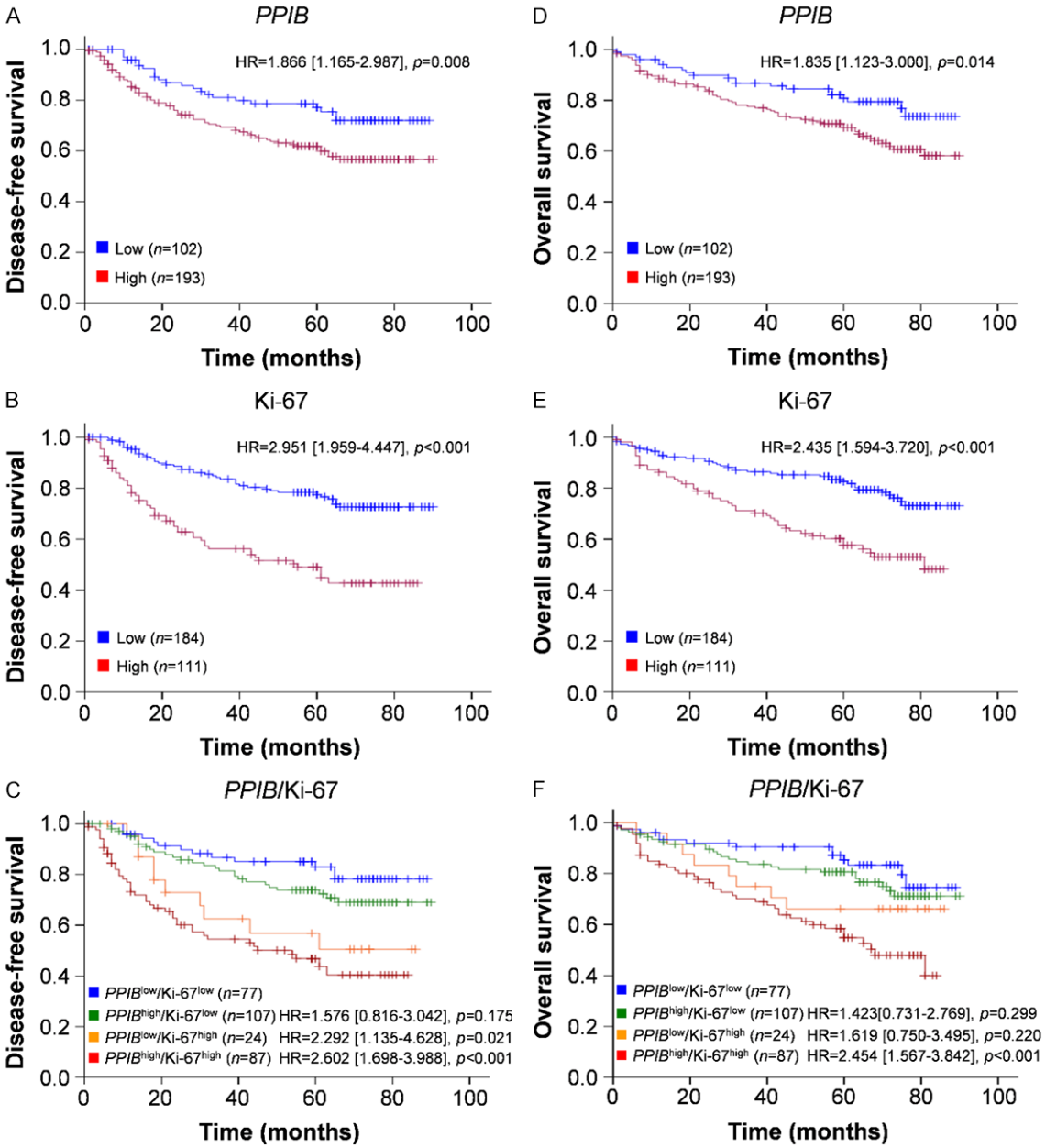

Figure 3. Kaplan-Meier survival analysis for PPIB and Ki-67 expression in adenocarcinoma patients. Patients with high PPIB (A, D) and high Ki-67 (B, E) expression showed poor disease-free (log rank *P*=0.008 and *P*<0.001, respectively) and overall survival rates (log rank *P*=0.014 and *P*<0.001, respectively) compared to patients with low expressions of both markers, respectively. A significant difference in survival rate was found among four groups (C, F), classified based on combined PPIB and Ki-67 expression (log rank *P*<0.001) and patients with $PPIB^{high}/Ki\text{-}67^{high}$ had worst disease-free (C) and overall survival rates (F).

ysis, high pT stage (hazard ratio [HR] 1.798, 95% CI 1.355-2.387, *P*<0.001) and high Ki-67 expression (HR 1.952, 95% CI 1.258-3.030, *P*=0.003) were independently associated with poor DFS. Old age (HR 1.033, 95% CI 1.07-1.059, *P*=0.012) and high pN stage (HR 2.816, 95% CI 1.780-4.453, *P*<0.001) was significantly associated with shorter OS. Notably, the combined expression of $PPIB^{high}/Ki\text{-}67^{high}$ was an independent prognosis factor for poor DFS (HR 1.424, 95% CI 1.177-1.723, *P*<0.001) and OS (HR 1.266, 95% CI 1.036-1.548, *P*=0.021).

Impact of PPIB/CypB silencing on oncogenic properties in NSCLC cells

Given that high PPIB expression is a poor prognostic factor in patients with ADC, we deter-

Table 3. Cox proportional univariate and multivariate analyses of disease-free survival in patients with pulmonary adenocarcinoma

Variables	Univariate analysis		Multivariate analysis		Multivariate analysis (including dual PPIB/Ki-67)	
	HR [95% CI]	*p* value	HR [95% CI]	*p* value	HR [95% CI]	*p* value
Age	0.991 [0.968-1.014]	0.419				
Sex	1.132 [0.752-1.704]	0.553				
pT	2.210 [1.706-2.862]	<0.001*	1.798 [1.355-2.387]	<0.001*	1.790 [1.350-2.374]	<0.001*
pN	2.734 [1.818-4.112]	<0.001*	1.531 [0.975-2.402]	0.064	1.532 [0.977-2.402]	0.063
PPIB^{high}	1.866 [1.165-2.987]	0.009*	1.550 [0.962-2.497]	0.072		
Ki-67^{high}	2.951 [1.959-4.447]	<0.001*	1.952 [1.258-3.030]	0.003*		
PPIB^{high}/Ki-67^{high}	2.161 [1.603-2.914]	<0.001*			1.424 [1.177-1.723]	<0.001*

HR, Hazard ratio; CI, confidence interval; *Statistically significant (P<0.05).

Table 4. Cox proportional univariate and multivariate analyses of overall survival in patients with pulmonary adenocarcinoma

Variables	Univariate analysis		Multivariate analysis		Multivariate analysis (including dual PPIB/Ki-67)	
	HR [95% CI]	*p* value	HR [95% CI]	*p* value	HR [95% CI]	*p* value
Age	1.037 [1.011-1.063]	0.005*	1.033 [1.007-1.059]	0.012*	1.033 [1.007-1.059]	0.012*
Sex	1.591 [1.025-2.469]	0.038*	1.317 [0.836-2.073]	0.235	1.293 [0.822-2.031]	0.266
pT	1.600 [1.223-2.093]	0.001*	1.217 [0.906-1.633]	0.192	1.206 [0.899-1.618]	0.211
pN	3.680 [2.410-5.620]	<0.001*	2.840 [1.791-4.503]	<0.001*	2.816 [1.780-4.453]	<0.001*
PPIB^{high}	1.835 [1.123-3.000]	0.015*	1.557 [0.948-2.559]	0.080		
Ki-67^{high}	2.435 [1.594-3.72]	<0.001*	1.447 [0.912-2.296]	0.116		
PPIB^{high}/Ki-67^{high}	1.524 [1.266-1.833]	<0.001*			1.266 [1.036-1.548]	0.021*

HR, Hazard ratio; CI, confidence interval; *Statistically significant (P<0.05).

mined the PPIB/CypB levels in NSCLC cells (A549, PC-9, Calu-3, H460 and H2009), including those derived from pulmonary ADC. Immortalized HBE BEAS-2B cells and non-transformed HBE 1799 cells were used as control cell lines. PPIB/CypB was highly expressed in all cancer cells compared to normal HBE cells (**Figure 4A**). To verify the role of PPIB/CypB in cancer cell proliferation, we transfected siRNAs targeting *PPIB* (*siPPIB-#1*, *-#2* or *-#3*) into H460 and PC-9 cells with high levels of PPIB/CypB (Supplementary Figure 4A and **Figure 4B**) and cellular Ki-67 levels were monitored. Silencing PPIB/CypB expression in H460 cells led to a significant reduction in cellular Ki-67 levels compared to *siGFP*-treated cells (Supplementary Figure 4B and **Figure 4C**). Consistently, *siPPIB*-treated PC-9 cells contained fewer proliferating cells than *siGFP*-treated cells as measured by Ki-67 staining (**Figure 4C**). In addition, the proliferation of *siPPIB*-treated cells was significantly lower than that of *siGFP*-treated cells (**Figure 4D**). Silencing of PPIB significantly decreased the colony formation efficacy and migration capacity of H460 and PC-9 cells compared with that of *siGFP*-treatment (**Figure 4E** and **4F**). These results demonstrate that PPIB/CypB may play a key role in the proliferation, colony formation, and migration of NSCLC cells.

Effect of PPIB/CypB overexpression on oncogenic properties in NSCLC and HBE cells

To further evaluate the effects of PPIB/CypB on cell proliferation, the PPIB/CypB expression vector or control vector (no insert) was transfected into H2009 and 1799 cells, which have low levels of PPIB/CypB (**Figure 5A**). Flow cytometry assays demonstrated that cellular Ki-67 levels were significantly increased in PPIB/CypB-overexpressing cells compared to those in the mock-control groups (**Figure 5B**). In addition, overexpression of PPIB/CypB promoted cell proliferation, colony formation, and migration of H2009 and 1799 cells (**Figure 5B-E**). These data indicate that PPIB/CypB expression alone is sufficient to promote the proliferation, colony formation, and migration of pulmonary ADC and HBE cells.

Discussion

Although initially known to facilitate immunosuppression, CypB has recently been reported to be expressed in various carcinomas and

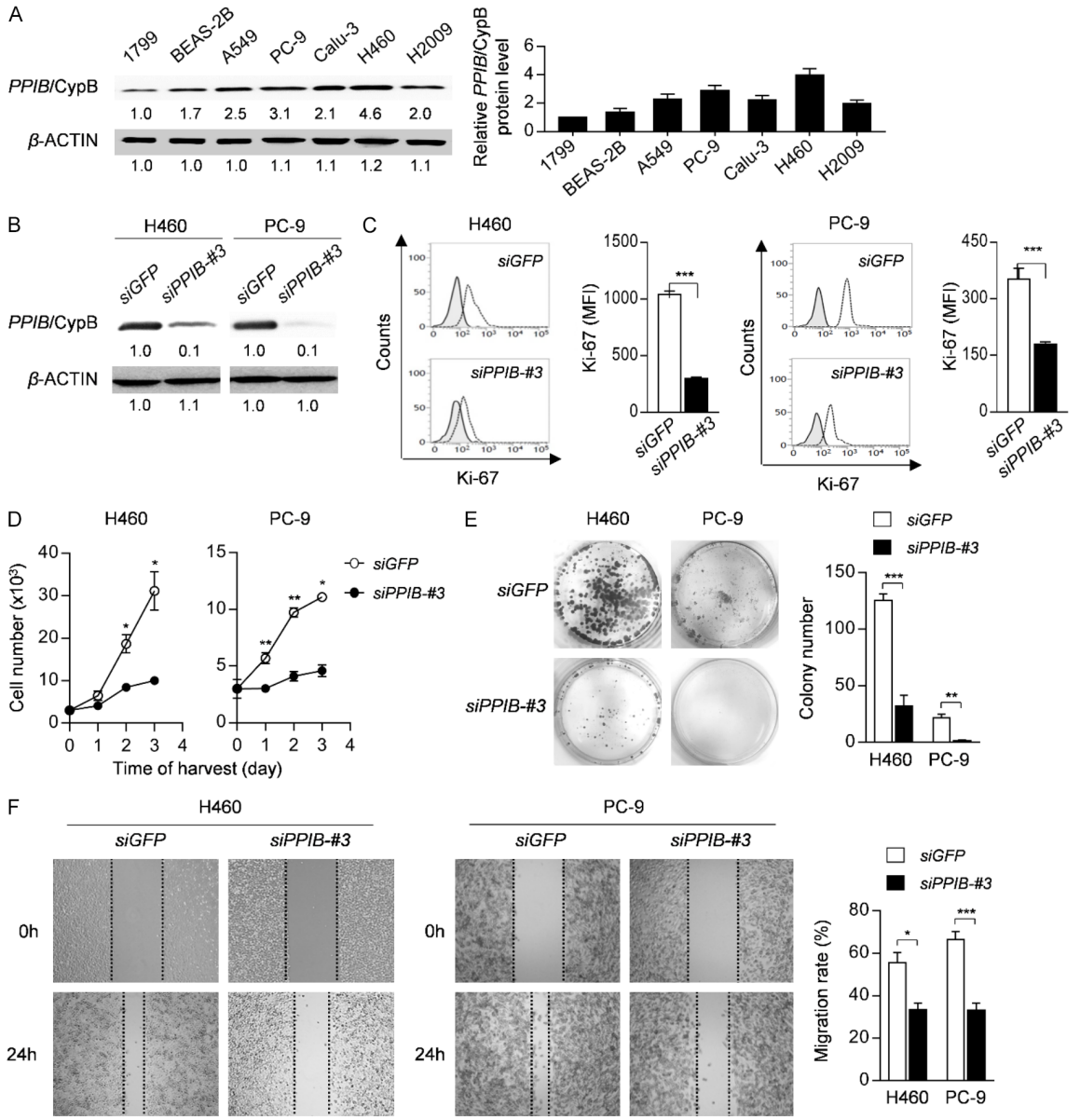

Figure 4. The impact of suppressing PPIB on the proliferation, colony formation, and migration of human NSCLC cells. (A) Protein level of PPIB in HBE cells (1799 and BEAS-2B) and NSCLC cells (A549, PC-9, Calu-3, H460 and H2009) was determined by Western blot. β-ACTIN was included as an internal loading control. Numbers below blot images indicate the expression as measured by fold change. Graph depicts the experimental quantitation based on at least three independent experiments. (B-F) H460 and PC-9 cells were transfected with specific siRNA for *GFP* (*siGFP*) or *PPIB* (*siPPIB-#3*). (B) PPIB protein level in these cells was determined by Western blot. β-ACTIN was included as an internal loading control. Numbers below blot images indicate the expression as measured by fold change. (C) The proliferation index of these cells, as measured by the mean fluorescence intensity of Ki-67 staining. Graphs represent three independent experiments performed in triplicate (*n*=3). (D) Proliferation rate of these cells. Cells were harvested at the indicated times and counted after trypan blue staining to exclude dead cells. (E) Colony formation assay. 500 cells were plated in 12 well plates and cultured for 1 week and formed colonies were stained with crystal violet. (F) The migration ability of these cells was measured using the wound healing assays. After scratching the confluent cell layer by using pipette tips, photographs were taken at 24 h. All experiments were performed in triplicate. **P*<0.05, ***P*<0.01 and ****P*<0.001 by student's t-test (two-tailed, unpaired) (C-F). Data represent the mean ± SD.

plays an important role in the malignant progression of tumors [15]. In NSCLC, it has been reported that CypB promotes cell proliferation, migration, invasion, and angiogenesis [23]. Because the *PPIB* gene, which encodes CypB, is expressed at a sufficiently low level, it is com-

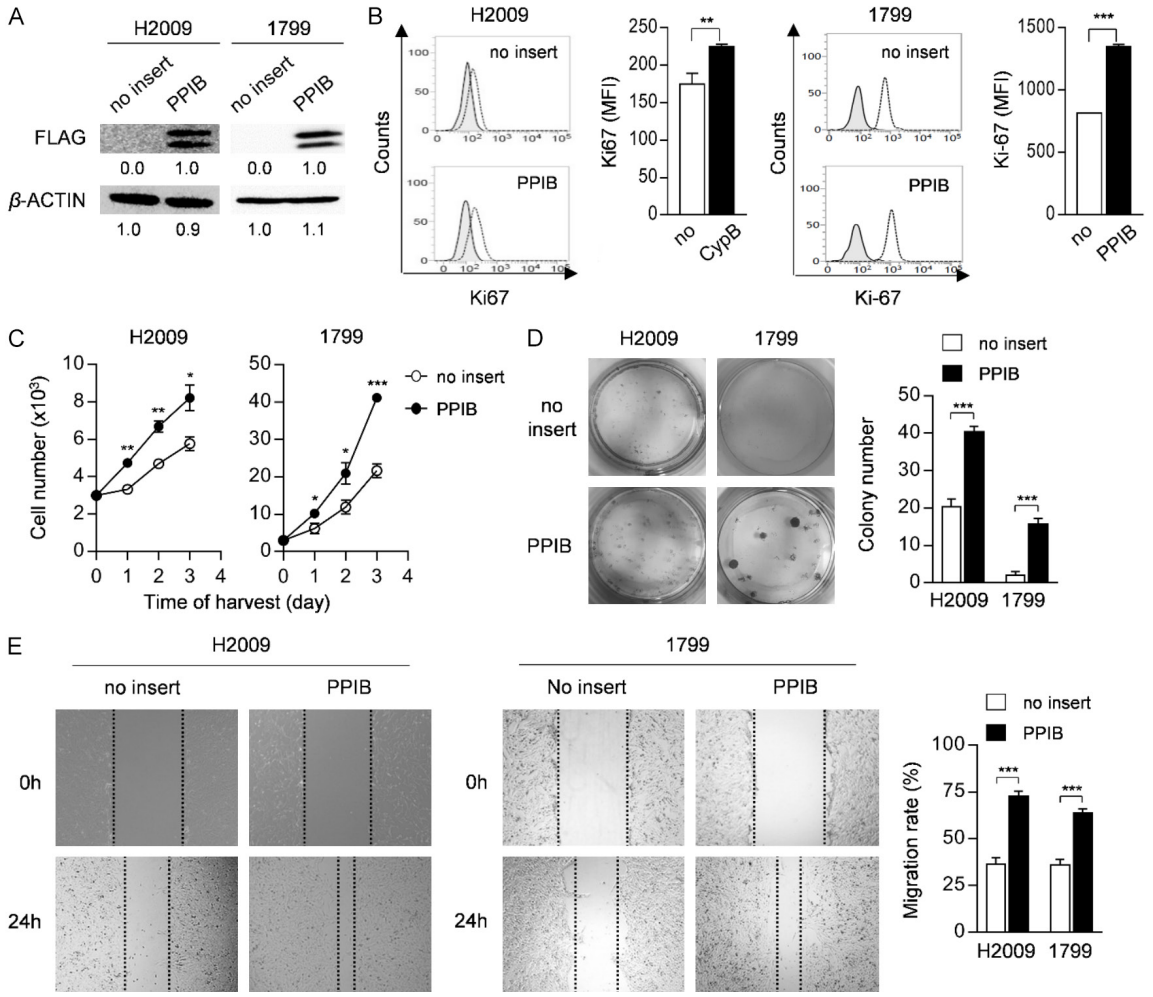

Figure 5. The effect of overexpressing PPIB on the proliferation, colony formation, and migration of NSCLC and HBE cells. H2009 and 1799 cells were stably transfected with empty vector (no insert) or PPIB expression vector. (A) FLAG-PPIB protein level in these cells was determined by Western blot. β-ACTIN was included as an internal loading control. The numbers below blot images indicate the expression as measured by fold change. (B) The proliferation index of these cells, as measured by the mean fluorescence intensity of Ki-67 staining. Graphs represent three independent experiments performed in triplicate (n=3). (C) Proliferation rate of these cells. Cells were harvested at the indicated times and counted after trypan blue staining to exclude dead cells. (D) Colony formation assay. 500 cells were plated in 12 well plates and cultured for 1 week and formed colonies were stained with crystal violet. (E) The migration ability of these cells was measured using the wound healing assays. After scratching the confluent cell layer by using pipette tips, photographs were taken at 24 h. All experiments were performed in triplicate. *P<0.05, **P<0.01 and ***P<0.001 by student's t-test (two-tailed, unpaired) (B-E). Data represent the mean ± SD.

monly used as a positive control gene to evaluate RNA quality and is frequently employed as a reference in RT-PCR. However, the clinicopathological significance of PPIB expression in NSCLC tissues has not been studied. In this study, we observed PPIB expression in formalin-fixed paraffin-embedded NSCLC tissues using a recently introduced non-radioisotopic RNA-ISH technology, RNAscope™, and quantified PPIB signals using computational approaches. This is the first study to analyze the correlation between clinicopathological findings and RNA expression levels of PPIB in NSCLC tissues, which reflect both genetic and epigenetic aberrations.

The detailed mechanism of action of PPIB/CypB in carcinogenesis has not yet been fully elucidated. It has been reported that PPIB/CypB is crucial for proliferation and colony formation and migration of various cancer cells [12, 23-25]. Previously, Teng et al. demonstrated that CypB expression was significantly higher in NSCLC tissues than in adjacent normal samples. CypB has also been reported to promote cell proliferation, migration, invasion, and

angiogenesis by regulating the signal transducer and activator of the transcription 3 (STAT3) pathway, a critical transcription factor that regulates cellular apoptosis, proliferation, and metastasis by modulating gene expression [23]. Jeong et al. presented that hypoxia induces CypB through the activation of transcription factor 6 in gastric adenocarcinoma [26] and Kim et al. reported that CypB induced by hypoxia stimulates the survival of hepatocellular carcinoma via a positive feedback loop with HIF-1α [17]. Consistent with previous reports, we observed that knockdown of CypB expression using CypB-targeted siRNA effectively suppressed lung cancer cell proliferation, colony formation, and migration. Additionally, the overexpression of CypB in HBE cells promoted cell proliferation, colony formation, and migration. These results suggest that CypB plays a crucial role in both the tumorigenesis and progression of lung cancer within these cell lines. The lung cancer cell lines used in this study included four isolates from ADC (A549, PC-9, Calu-3, and H2009) and one (H460) from a large cell carcinoma. Interestingly, H460 cells exhibited the highest levels of PPIB as indicated by western blot analysis. Further studies are required to investigate the clinical impact of PPIB expression in other histological subtypes of lung cancer.

The Ki-67 proliferation index, determined using immunohistochemistry, is extensively utilized to assess tumor cell proliferation [27] and holds prognostic and predictive value in various cancers, including pulmonary adenocarcinoma [28-31]. In this study, we aim to investigate the potential correlation between PPIB and Ki-67 in NSCLC patient samples. There is a significant correlation between PPIB expression and Ki-67 index in NSCLC tissues. Additionally, heightened PPIB and Ki-67 expression levels were significantly linked to clinical variables associated with poor outcomes, especially ADC. Furthermore, our results revealed that $PPIB^{high}$/$Ki\text{-}67^{high}$ was an independent indicator of poor prognosis in pulmonary ADC but not in SCC. From the perspective of pathogenesis and associated molecular alterations in lung cancer, ADC differs from SCC. ADC may arise from basally differentiated or undifferentiated stem cells in the peripheral compartment, whereas SCC may arise from cells in the central compartment. Due to distinct treatment options, molecular alterations, and clinical features of ADC and SCC, proper histological classification is of increasing importance. The prognostic impact of $PPIB^{high}$/$Ki\text{-}67^{high}$ and the association between high PPIB expression and advanced stage, disease recurrence, and patient mortality, seen exclusively in ADC, may suggest that the role of PPIB/CypB in NSCLC progression also differs between ADC and SCC. Only a few studies have investigated the effect of CypB expression on the clinical outcomes of patients with cancer. In colon cancer, it has been reported that overexpression of CypB is an independent prognostic indicator of poor survival, and CypB is involved in tumor metastasis-associated signaling pathways [24].

Meta-analyses of numerous studies performed on resected NSCLC have suggested that high Ki-67 values are correlated with poor prognosis and shorter DFS [7]. However, the informative value of studies on this issue is limited by the different Ki-67 clones, use of various Ki-67 cut-off points, and study cohorts with mixed histology [32]. We determined that the most discriminative Ki-67 cut-off point was 23%. Using these cutoff points, significant correlations were observed between high Ki-67 expression and clinicopathological characteristics, including male sex, smoking history, poor differentiation, higher tumor stage, and poor outcome of all NSCLC (Supplementary Table 1) and ADC (**Table 1**). Notably, Ki-67 was more frequently expressed in SCC than in ADC ($P<0.001$; Supplementary Figure 2). However, using a cut-off point of 23%, there was no association between Ki-67 expression and clinicopathological findings in SCC. Moreover, we did not find the most powerful Ki-67 cut-off value for SCC. Therefore, we conclude that high Ki-67 expression is meaningful in ADC but not in SCC, and that Ki-67 expression varies according to histology. Similarly, a recent study found that Ki-67 was a highly significant and independent predictor of DFS for pulmonary ADC and adenosquamous carcinoma, but not for SCC [31].

A limitation of this study is that it was a single-institute cohort study, and only a small number of patients with stage IV disease were included because only surgically resected NSCLC specimens were collected. Further studies in larger cohorts may provide insights into the role of PPIB in the carcinogenesis of NSCLC with heterogeneous clinical characteristics.

In conclusion, we demonstrated that the overexpression of PPIB/CypB promoted the proliferation, colony formation, and migration of NSCLC cells. Additionally, we report for the first time that high PPIB expression as well as high Ki-67 expression is significantly associated with poor DFS and OS in pulmonary ADC but not in SCC. Notably, combined $PPIB^{high}$/$Ki\text{-}67^{high}$ expression serves as an independent prognostic factor for both DFS and OS, particularly in ADC. These findings suggest that PPIB/CypB has the potential to be a therapeutic target and prognostic indicator for pulmonary ADC.

Acknowledgements

This work was supported in part by the research promoting grant from Keimyung University Dongsan Medical Center in 2017.

Disclosure of conflict of interest

None.

Address correspondence to: Dr. Jeong Won Kim, Department of Pathology, Kangnam Sacred Heart Hospital, Hallym University College of Medicine, Shingilro-1, Yeongdeungpo-gu, Seoul 07441, Republic of Korea. Tel: +82-2-829-5267; ORCID: 0000-0002-6552-9875; E-mail: jwkim@hallym.or.kr; Dr. Joon-Yong Chung, Molecular Imaging Branch, Center for Cancer Research, National Cancer Institute, National Institutes of Health, MSC1500, Bethesda, MD 20892, USA. Tel: 1-240-760-7172; ORCID: 0000-0001-5041-5982; E-mail: chungjo@mail.nih.gov

References

[1] Siegel RL, Miller KD, Wagle NS and Jemal A. Cancer statistics, 2023. CA Cancer J Clin 2023; 73: 17-48.

[2] Ganti AK, Klein AB, Cotarla I, Seal B and Chou E. Update of incidence, prevalence, survival, and initial treatment in patients with non-small cell lung cancer in the US. JAMA Oncol 2021; 7: 1824-1832.

[3] Rami-Porta R, Asamura H, Travis WD and Rusch VW. Lung cancer - major changes in the American Joint Committee on Cancer eighth edition cancer staging manual. CA Cancer J Clin 2017; 67: 138-155.

[4] Hou S, Zhou S, Qin Z, Yang L, Han X, Yao S and Ji H. Evidence, mechanism, and clinical relevance of the transdifferentiation from lung adenocarcinoma to squamous cell carcinoma. Am J Pathol 2017; 187: 954-962.

[5] Yun JK, Kwon Y, Kim J, Lee GD, Choi S, Kim HR, Kim YH, Kim DK and Park SI. Clinical impact of histologic type on survival and recurrence in patients with surgically resected stage II and III non-small cell lung cancer. Lung Cancer 2023; 176: 24-30.

[6] Phruttinarakorn B, Reungwetwattana T and Incharoen P. Association of histologic subtypes with genetic alteration and PD-L1 expression in pulmonary adenocarcinoma. Mol Clin Oncol 2020; 13: 12.

[7] Chirieac LR. Ki-67 expression in pulmonary tumors. Transl Lung Cancer Res 2016; 5: 547-551.

[8] Price ER, Zydowsky LD, Jin MJ, Baker CH, McKeon FD and Walsh CT. Human cyclophilin B: a second cyclophilin gene encodes a peptidyl-prolyl isomerase with a signal sequence. Proc Natl Acad Sci U S A 1991; 88: 1903-1907.

[9] Spik G, Haendler B, Delmas O, Mariller C, Chamoux M, Maes P, Tartar A, Montreuil J, Stedman K, Kocher HP, et al. A novel secreted cyclophilin-like protein (SCYLP). J Biol Chem 1991; 266: 10735-10738.

[10] Heitman J and Cullen BR. Cyclophilin B escorts the hepatitis C virus RNA polymerase: a viral achilles heel? Mol Cell 2005; 19: 145-146.

[11] Fang F, Flegler AJ, Du P, Lin S and Clevenger CV. Expression of cyclophilin B is associated with malignant progression and regulation of genes implicated in the pathogenesis of breast cancer. Am J Pathol 2009; 174: 297-308.

[12] Fang F, Zheng J, Galbaugh TL, Fiorillo AA, Hjort EE, Zeng X and Clevenger CV. Cyclophilin B as a co-regulator of prolactin-induced gene expression and function in breast cancer cells. J Mol Endocrinol 2010; 44: 319-329.

[13] Ram BM and Ramakrishna G. Endoplasmic reticulum vacuolation and unfolded protein response leading to paraptosis like cell death in cyclosporine A treated cancer cervix cells is mediated by cyclophilin B inhibition. Biochim Biophys Acta 2014; 1843: 2497-2512.

[14] Choi JW, Schroeder MA, Sarkaria JN and Bram RJ. Cyclophilin B supports Myc and mutant p53-dependent survival of glioblastoma multiforme cells. Cancer Res 2014; 74: 484-496.

[15] Meng DQ, Li PL and Xie M. Expression and role of cyclophilin B in stomach cancer. Genet Mol Res 2015; 14: 5346-5354.

[16] Hartmann E, Wollenberg B, Rothenfusser S, Wagner M, Wellisch D, Mack B, Giese T, Gires O, Endres S and Hartmann G. Identification and functional analysis of tumor-infiltrating plasmacytoid dendritic cells in head and neck cancer. Cancer Res 2003; 63: 6478-6487.

[17] Kim Y, Jang M, Lim S, Won H, Yoon KS, Park JH, Kim HJ, Kim BH, Park WS, Ha J and Kim SS.

Role of cyclophilin B in tumorigenesis and cisplatin resistance in hepatocellular carcinoma in humans. Hepatology 2011; 54: 1661-1678.
[18] Choi TG, Nguyen MN, Kim J, Jo YH, Jang M, Nguyen NNY, Yun HR, Choe W, Kang I, Ha J, Tang DG and Kim SS. Cyclophilin B induces chemoresistance by degrading wild-type p53 via interaction with MDM2 in colorectal cancer. J Pathol 2018; 246: 115-126.
[19] Tsao M, Asamura H, Borczuk A, Dacic S, Devesa S, Kerr K, MacMahon H, Rusch V, Samet J and Scagliotti G. Tumours of the lung: introduction. In: WHO classification of tumours: thoracic tumours/WHO Classification of Tumours Editorial Board. 2021; pp. 20-28.
[20] Okamoto K, Rausch JW, Wakashin H, Fu Y, Chung JY, Dummer PD, Shin MK, Chandra P, Suzuki K, Shrivastav S, Rosenberg AZ, Hewitt SM, Ray PE, Noiri E, Le Grice SFJ, Hoek M, Han Z, Winkler CA and Kopp JB. APOL1 risk allele RNA contributes to renal toxicity by activating protein kinase R. Commun Biol 2018; 1: 188.
[21] Noh KH, Kang TH, Kim JH, Pai SI, Lin KY, Hung CF, Wu TC and Kim TW. Activation of Akt as a mechanism for tumor immune evasion. Mol Ther 2009; 17: 439-447.
[22] Song KH, Choi CH, Lee HJ, Oh SJ, Woo SR, Hong SO, Noh KH, Cho H, Chung EJ, Kim JH, Chung JY, Hewitt SM, Baek S, Lee KM, Yee C, Son M, Mao CP, Wu TC and Kim TW. HDAC1 upregulation by NANOG promotes multidrug resistance and a stem-like phenotype in immune edited tumor cells. Cancer Res 2017; 77: 5039-5053.
[23] Teng MR, Huang JA, Zhu ZT, Li H, Shen JF and Chen Q. Cyclophilin B promotes cell proliferation, migration, invasion and angiogenesis via regulating the STAT3 pathway in non-small cell lung cancer. Pathol Res Pract 2019; 215: 152417.
[24] Zhang X, Tan J, Yang L and An G. Cyclophilin B overexpression predicts a poor prognosis and activates metastatic pathways in colon cancer. Transl Cancer Res 2020; 9: 3573-3585.
[25] Liu J, Zuo Y, Qu GM, Song X, Liu ZH, Zhang TG, Zheng ZH and Wang HK. CypB promotes cell proliferation and metastasis in endometrial carcinoma. BMC Cancer 2021; 21: 747.
[26] Jeong K, Kim K, Kim H, Oh Y, Kim SJ, Jo Y and Choe W. Hypoxia induces cyclophilin B through the activation of transcription factor 6 in gastric adenocarcinoma cells. Oncol Lett 2015; 9: 2854-2858.
[27] Gerdes J, Li L, Schlueter C, Duchrow M, Wohlenberg C, Gerlach C, Stahmer I, Kloth S, Brandt E and Flad HD. Immunobiochemical and molecular biologic characterization of the cell proliferation-associated nuclear antigen that is defined by monoclonal antibody Ki-67. Am J Pathol 1991; 138: 867-873.
[28] Pelosi G, Rindi G, Travis WD and Papotti M. Ki-67 antigen in lung neuroendocrine tumors: unraveling a role in clinical practice. J Thorac Oncol 2014; 9: 273-284.
[29] Li Z, Li F, Pan C, He Z, Pan X, Zhu Q, Wu W and Chen L. Tumor cell proliferation (Ki-67) expression and its prognostic significance in histological subtypes of lung adenocarcinoma. Lung Cancer 2021; 154: 69-75.
[30] Roge R, Nielsen S, Riber-Hansen R and Vyberg M. Ki-67 proliferation index in breast cancer as a function of assessment method: a NordiQC experience. Appl Immunohistochem Mol Morphol 2021; 29: 99-104.
[31] Warth A, Cortis J, Soltermann A, Meister M, Budczies J, Stenzinger A, Goeppert B, Thomas M, Herth FJ, Schirmacher P, Schnabel PA, Hoffmann H, Dienemann H, Muley T and Weichert W. Tumour cell proliferation (Ki-67) in non-small cell lung cancer: a critical reappraisal of its prognostic role. Br J Cancer 2014; 111: 1222-1229.
[32] Lee JS, Yoon A, Kalapurakal SK, Ro JY, Lee JJ, Tu N, Hittelman WN and Hong WK. Expression of p53 oncoprotein in non-small-cell lung cancer: a favorable prognostic factor. J Clin Oncol 1995; 13: 1893-1903.

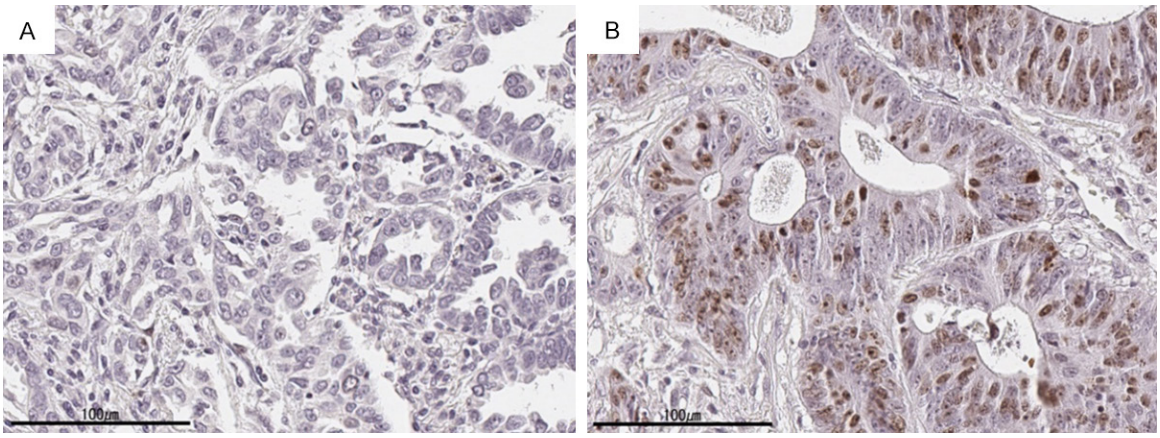

Supplementary Figure 1. Representative low (A) and high (B) Ki-67 immunohistochemical expressions in pulmonary adenocarcinoma.

Supplementary Table 1. Association of *PPIB* and Ki-67 expression with clinicopathologic characteristics in human NSCLC

Category (*n*=431)	*PPIB*, No. (%)			Ki-67, No. (%)		
	Low (*n*=152)	High (*n*=279)	*p* value	Low (*n*=185)	High (*n*=246)	*p* value
Age	62.4 ± 8.7	63.5 ± 9.5	0.246	61.5 ± 9.1	64.3 ± 9.1	0.002*
Sex			0.302			<0.001*
Male	100 (65.8)	197 (70.6)		87 (47.0)	210 (85.4)	
Female	52 (34.2)	82 (29.4)		98 (53.0)	36 (14.6)	
Smoking			0.280			<0.001*
No	58 (38.2)	92 (33.0)		110 (59.5)	40 (16.3)	
Yes	94 (61.8)	187 (67.0)		75 (40.5)	206 (83.7)	
Histologic type			0.659			<0.001*
AD	102 (67.1)	193 (69.2)		184 (99.5)	111 (45.1)	
SqCC	50 (32.9)	86 (30.8)		1 (0.6)	135 (54.9)	
pT stage			0.131			<0.001*
Ia-Ic	73 (48.0)	119 (42.7)		114 (61.6)	78 (31.7)	
IIa-IIb	51 (33.6)	90 (32.2)		53 (28.6)	88 (35.8)	
III-IV	28 (18.4)	70 (25.1)		18 (9.7)	80 (32.5)	
pN stage			0.052			<0.001*
0	113 (74.3)	182 (65.2)		150 (81.1)	145 (58.9)	
I-II	39 (25.7)	97 (34.8)		35 (18.9)	101 (41.1)	
pM stage			0.028*			0.401
M0	150 (98.7)	263 (94.3)		179 (96.8)	234 (95.1)	
M1	2 (1.3)	16 (5.7)		6 (3.29)	12 (4.92)	
Stage			0.015*			<0.001*
I	93 (61.2)	148 (53.0)		138 (74.6)	103 (41.9)	
II	31 (20.4)	51 (18.3)		18 (9.77)	64 (26.0)	
III	26 (17.1)	64 (22.9)		23 (12.4)	67 (27.2)	
IV	2 (1.3)	16 (5.7)		6 (3.24)	12 (4.87)	
Recurrence			0.044*			0.001*
Absent	114 (75.0)	183 (65.5)		143 (77.3)	154 (62.6)	
Present	38 (25.0)	96 (34.4)		42 (22.7)	92 (37.4)	
Status			0.006*			<0.001*
Alive	116 (76.3)	177 (63.4)		145 (78.4)	148 (60.2)	
Expire	36 (23.6)	102 (36.5)		40 (21.6)	98 (39.8)	

NSCLC, non-small cell lung cancer; AD, adenocarcinoma; SqCC, squamous cell carcinoma. *Statistically significant ($P<0.05$).

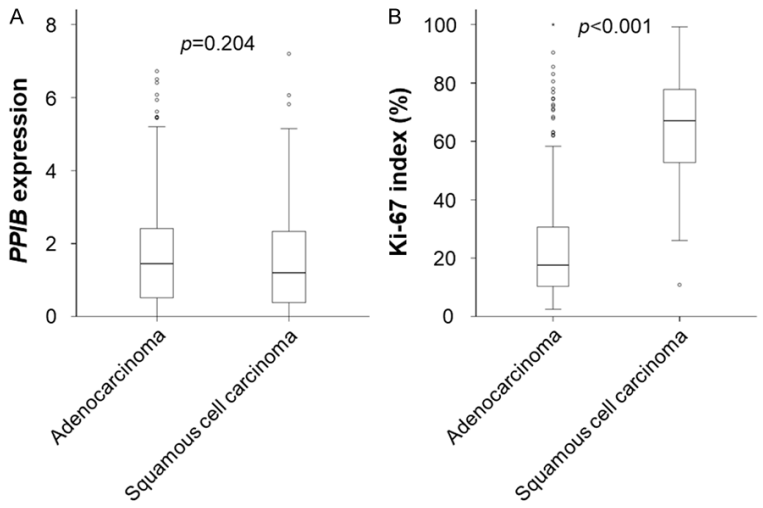

Supplementary Figure 2. PPIB and Ki-67 expressions in pulmonary adenocarcinoma (ADC) and squamous cell carcinoma (SCC). (A) The median value of PPIB expression in ADC is 1.45 (range 0.50-2.42) and in SCC was 1.20 (range 0.39-2.33), showing no significant difference. However, (B) Ki-67 expression was more frequently observed in SCC (median 66.99, range 52.73-77.95) than in ADC (median 17.67, range 10.31-30.67) (*P*<0.001).

Supplementary Table 2. Association of *PPIB* and Ki-67 expression with clinicopathologic characteristics in pulmonary squamous cell carcinoma

Category	*PPIB*, No. (%)				Ki-67, No. (%)			
	No	Low (*n*=50)	High (*n*=86)	*p* value	No	Low (*n*=1)	High (*n*=135)	*p* value
Age	136	63.6 ± 8.6	66.6 ± 7.7	0.038*	136	73.0 ± NA	65.5 ± 8.2	
Sex				0.368				1.000
Male	135	49 (98.0)	86 (100.0)		135	1 (100.0)	134 (99.3)	
Female	1	1 (2.0)	0		1	0	1 (0.7)	
Smoking				1.000				1.000
No	4	1 (2.0)	3 (3.5)		4	0	4 (3.0)	
Yes	132	49 (98.0)	83 (96.5)		132	1 (100.0)	131 (97.0)	
Differentiation				0.655				0.784
Well	11	3 (6.0)	8 (9.3)		11	0	11 (8.1)	
Moderate	94	38 (76.0)	56 (65.1)		94	1 (100.0)	93 (68.9)	
Poor	31	9 (18.0)	22 (25.6)		31	0	31 (23.0)	
pT stage				0.124				0.424
Ia-Ic	36	15 (30.0)	21 (24.4)		36	0	36 (26.7)	
IIa-IIb	42	19 (38.0)	23 (26.8)		42	0	42 (31.1)	
III-IV	58	16 (32.0)	42 (48.8)		58	1 (100.0)	57 (42.2)	
pN stage				0.783				0.375
0	85	32 (64.0)	53 (61.6)		85	0	85 (63.0)	
I-II	51	18 (36.0)	33 (38.4)		51	1 (100.0)	50 (37.0)	
pM stage				0.158				1.000
M0	131	50 (100.0)	81 (94.2)		131	1 (100.0)	130 (96.3)	
M1	5	0	5 (5.8)		5	0	5 (3.7)	
Stage				0.388				0.227
I	54	22 (44.0)	32 (37.2)		54	0	54 (40.0)	
II	43	14 (28.0)	29 (33.7)		43	0	43 (31.9)	
III	34	14 (28.0)	20 (23.3)		34	1 (100.0)	33 (24.4)	
IV	5	0)	5 (5.8)		5	0	5 (3.7)	

Recurrence				0.909				0.294
Absent	96	35 (70.0)	61 (70.9)		96	0	96 (71.1)	
Present	40	15 (30.0)	25 (29.1)		40	1 (100.0)	39 (28.9)	
Status				0.168				0.375
Alive	85	35 (70.0)	50 (58.1)		85	0	85 (63.0)	
Expire	51	15 (30.0)	36 (41.9)		51	1 (100.0)	50 (37.0)	

*Statistically significant (P<0.05).

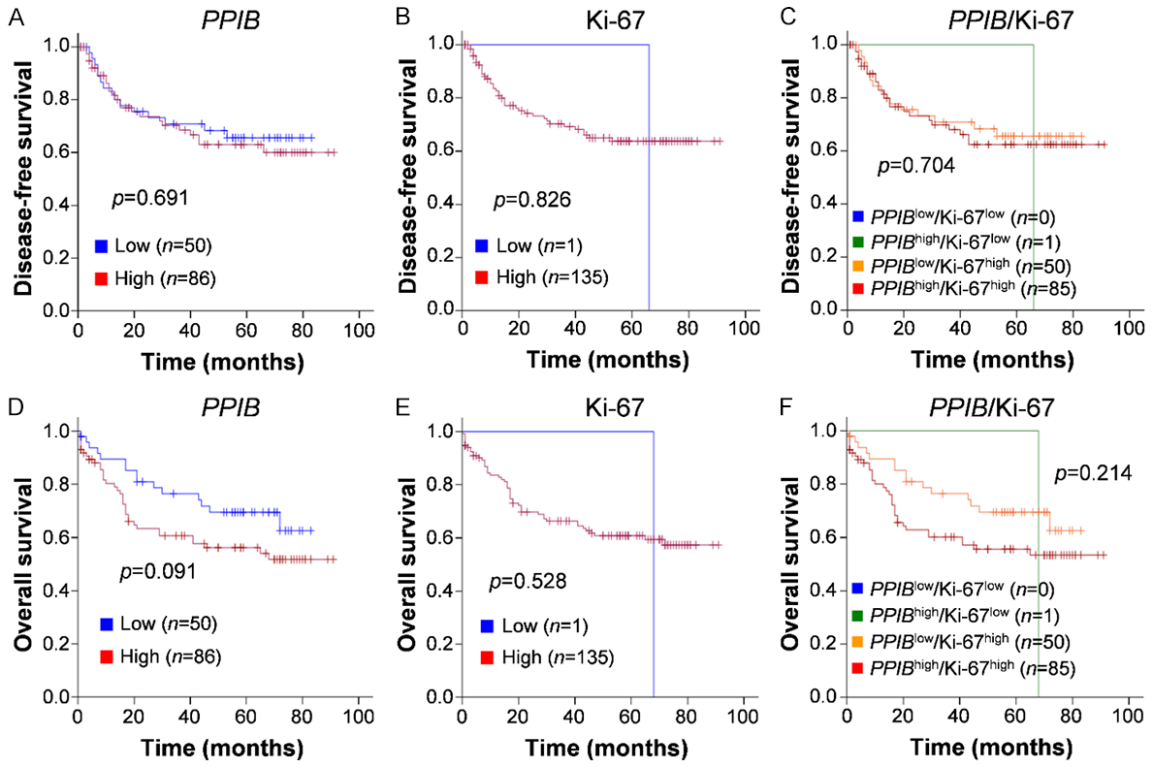

Supplementary Figure 3. Kaplan-Meier survival curves for PPIB and Ki-67 expression in squamous cell carcinoma patients. No significant differences in disease-free and overall survival were observed for PPIB (P=0.691 and 0.091, respectively) (A, D), Ki-67 (P=0.826 and 0.528, respectively) (B, E), and combined PPIB and Ki-67 expressions (P=0.704 and 0.214, respectively) (C, F).

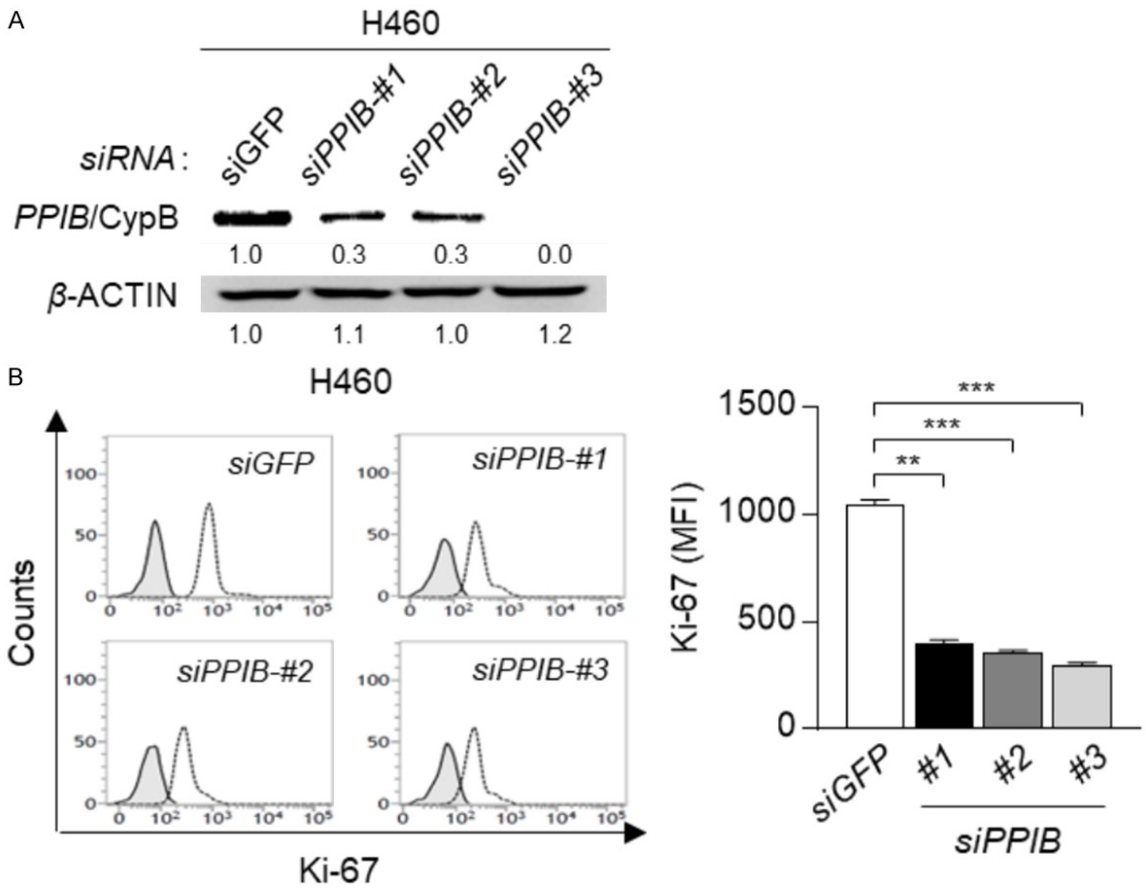

Supplementary Figure 4. Silencing of PPIB decreases cellular Ki-67 level of H460 NSCLC cells. H460 cells were transfected with *siGFP*, *siPPIB* #1, #2, or #3. A. Protein level of PPIB was determined by Western blot. *β*-ACTIN was included as an internal loading control. The numbers below blot images indicate the expression as measured by fold change. B. The proliferation index of these cells, as measured by the mean fluorescence intensity of Ki-67 staining. Graphs represent three independent experiments performed in triplicate (n=3). $^{**}P<0.01$ and $^{***}P<0.001$, by one-way ANOVA. Data represent the mean ± SD.